Gene expression study in the juvenile mouse testis: identification of stage-specific molecular pathways during spermatogenesis

Emily J. Clemente,[1] Robert A. Furlong,[1] Kate L. Loveland,[2] Nabeel A. Affara[1]

[1]Department of Pathology, University of Cambridge, Tennis Court Road, Cambridge CB2 1QP, United Kingdom
[2]Monash Institute of Medical Research and The Australian Research Council Centre of Excellence in Biotechnology and Development, Monash University, Clayton, Victoria 3168, Australia

Abstract

A gene expression time course in the juvenile mouse testis was established using cDNA microarrays derived from a variety of isolated testis cell types. In conjunction with the use of four germ cell-deficient mouse models, a stage and cell-type classification over nine time points has been obtained and analyzed for differential expression of genes. The expression profiles have been clustered into nine groups and subjected to detailed analysis of associated gene ontology. This has allowed the correlation of particular cellular processes and functions with different expression clusters. Focused analysis of transcripts involved in cell number regulation (apoptosis and proliferation) and their spatiotemporal expression patterns are presented. The findings indicate that for genes involved in both apoptosis and proliferation, several distinct pathways regulating these processes are active in somatic and germ cell lineages.

Introduction

Spermatogenesis is a complex cyclical process leading to the formation of mature spermatozoa. Germ cells undergo a series of unique stage-specific events including meiotic division, genetic recombination, haploid gene expression, radical remodeling and condensation of chromatin, and profound morphologic differentiation resulting in the formation of new structures characteristic of mature sperm (Braun 1998; Cohen and Pollard 2001; Pawlowski and Cande 2005; Poccia 1986). The regulation of this highly ordered process involves an evolutionarily conserved program of gene expression in germ cells (Eddy 2002; Handel 1987; Hecht 1998). Sertoli cells are a key element in the coordination of the effects of this intrinsic program, facilitating signaling between germ cells at different stages of spermatogenesis and their maintenance (Griswold 1995; Saunders 2003). A fundamental aspect of ongoing germ cell production is the achievement of the correct ratio of germ cells to Sertoli cells, established through a balance between spermatogonial proliferation and apoptosis during the first wave of spermatogenesis after birth (Rodriguez et al. 1997). Extrinsic influences on spermatogenesis are mediated through the actions of hormones (primarily testosterone and FSH) that modulate gene expression to establish and maintain a favorable environment for continued germ cell production (Holdcraft and Braun 2004; Meehan et al. 2000).

Although our knowledge of the molecular genetics of spermatogenesis is improving rapidly, unraveling its complexity remains a challenge. A fuller understanding will require more in-depth focus on specific pathways, building on the large-scale profiling projects of the last few years (Ellis et al. 2004; Maratou et al. 2004; Schultz et al. 2003; Sha et al. 2002; Shima et al. 2004). As highlighted in a recent review (Wrobel and Primig 2005), conclusions drawn regarding gene regulation and function will be greatly strengthened by the analysis of mice that display a specific fertility phenotype (see Chubb 1989; Cooke and Saunders 2002 for reviews of mouse models of interest).

Previous work by our group has characterized a subtracted testis-specific gene set (Ellis et al. 2004)

and used this to discover novel genes associated with abnormalities in later stages of spermatogenesis (Ellis et al 2005; Touré et al. 2005). This study by contrast examines the apoptotic and cell proliferation pathways involved in the control of cell numbers in the testis. The subtracted gene set is not suitable for this analysis because genes involved in widespread cellular processes such as proliferation and apoptosis are removed during the subtraction process. Thus, the gene set used here is a set of testis cell type-specific unsubtracted cDNA libraries (McCarrey et al. 1999; see *Materials and methods*). This specifically targets the early germ cell and somatic cell types in which most apoptosis and cell proliferation occurs. The use of a gene set derived from the tissue under consideration ensures that the most appropriate transcript variants are present on the array and enables the discovery of novel genes which may not be present in nontargeted gene sets.

Expression profiling of the first wave of spermatogenesis and a series of germ cell-deficient mouse models was used to characterize the cDNA gene set, and *in situ* hybridization was used to confirm assignment of genes to particular cell types. Subsequently, gene ontology analysis was used to analyze the cellular processes occurring in gene clusters assigned to specific cell types, and RT-PCR analysis was used to confirm and extend the data on genes related to apoptosis and cell proliferation.

These data have been analyzed (1) to classify expression profiles into nine clusters and to associate these clusters with detailed gene ontology and (2) to identify genes that influence pathways of apoptosis and proliferation. The networks of genes involved in these biological processes were shown to be expressed in both germ and somatic cell types in a stage-specific manner.

Materials and methods

Sample collection. Two biological replicate samples of whole testes were collected from C57BL6J normal mice at different ages postpartum (1, 5, 10, 13, 15, 19, 23, 35, 56 days) in agreement with ASPA 86 Act (Animal Scientific Procedures Act) of Parliament under Home Office licence PIL80/7029. The testicular samples were immediately snap-frozen in isopentane on dry ice and stored at −80°C. Eight-week-old whole testes for *mshi*, *Bax−/−*, and *bs* (all C57BL6J) and their respective controls (homozygous normal or unaffected heterozygous) were obtained from The Jackson Laboratory (Bar Harbor, ME). XX*Sxr*[b] and its control paired testes (albino MF1

strain) were obtained from Dr. Paul Burgoyne at the National Institute for Medical Research, Mill Hill, UK.

Mutant mouse strains. As for our prior work, four mutant mouse strains with variant germ cell compositions were used to refine the assignment of genes to cell type. These were (1) the XX*Sxr*[b] mouse with a complete lack of germ cells (Mazeyrat et al. 2001; McLaren and Monk 1981), (2) the *mshi* mutation that leads to a mouse with dysfunctional Sertoli cells and germ cells that do not progress beyond meiotic stages (Ward-Bailey et al. 1996), (3) the *Bax−/−* "knockout" mouse where there is accumulation of atypical spermatogonia, eliminated later in adulthood, and absence of haploid cells (Knudson et al. 1995), and (4) the *bs* (blind sterile) mouse which displays all germ cells types, though in reduced number, and abnormal spermatozoa due to acrosome assembly failure (Varnum 1983). All mouse models were analyzed at 8 weeks postpartum.

RNA extraction. Testes from the same time point (or mouse model) were pooled for each biological replicate to obtain sufficient material for RNA extraction using TRIzol reagent in accordance with the manufacturer's protocol (Invitrogen, Carlsbad, CA), followed by column purification (RNeasy, Qiagen, Valencia, CA). RNA quality was assessed with the Lab-on-a-chip system (Agilent, Palo Alto, CA).

Microarrays. cDNA clone insert DNA for arraying were derived from six testis purified-cell-type libraries. These correspond to IMAGE clone plate numbers 8825−8830 (day 8 type B spermatogonia), 8831−8836 (day 18 mixed primary spermatocytes), 8846−8850 (adult round spermatids), 9339−9342 (day 8 type A spermatogonia), 13,869−13,871 (day 6 primitive type A spermatogonia), and 13,872−13,874 (day 18 Sertoli cells) (McCarrey et al. 1999). The cDNA clone inserts and positive and negative controls were spotted in triplicate using a BioRobotics Microgrid II arrayer. In total, 10,367 testis cDNA clones, corresponding to at least 3627 different genes, were arrayed. However, sequencing of the library is still ongoing and therefore it is likely that the gene diversity is higher (3203 clones remain with no sequence information available).

Hybridizations and data capture. Four technical and two biological replicate hybridizations were performed for each time point. All hybridizations were conducted in standard formamide-based buffer and reverse-transcribed cDNA from RNA popula-

Table 1. Proportion (%) of clones from purified cell-type libraries within each cluster

Library/ Cluster	S1 (23%)	S2 (52%)	PreM1 (105%)	PreM2 (18%)	M1 (37%)	M2 (26.5%)	PM1 (18%)	PM2 (22%)	PM3 (21.5%)
Sertoli cell (25%)	**71**	**39**	23	10	4	5	0	4.5	0.25
Prim Aspg (25%)		8	14	17	12	1	0.7	0	0.8
Aspg (35%)	3	5	9	16	1	7	3.5	2.2	4.5
Bspg (35%)	16	23	**46**	**59**	3	0.5	0	1	0.25
Spc (32%)	1	14	4	3	**59**	**49**	36.5	34.5	14
Spd (32%)	1	5	1	0	32	37.8	**60**	**57**	**78**

The level of redundancy in each library and cluster is indicated in parentheses.
Prim Apg = primitive type A spermatogonia; Aspg = type A spermatogonia; Bspg = type B spermatogonia; Spc = spermatocyte; Spd = spermatid. The nine clusters are named somatic (S1, S2), premeiotic (PreM1, PreM2), meiotic (M1, M2), and postmeiotic (PM1, PM2, PM3).

tions were labeled with either Cy3 or Cy5 using the indirect amino allyl approach (Ellis et al. 2004). Control and test cDNA populations were labeled with Cy3 and Cy5, respectively. All time points were directly compared with the same control (8-week-old adult mouse testis RNA), also corresponding to the final time point. The mutant mouse models were compared with their age-matched controls. After hybridization, slides were washed for 10 min at room temperature in decreasing strengths of Saline Sodium Citrate (SSC) (1/0.5/0.1 ×). A CCD scanner (ArrayWorX) was used to measure spot intensities of all slides and the resulting .tiff files were quantitated using Bluefuse software (BlueGnome, Cambridge, UK).

Data analysis. Normalization was performed to a panel of relatively invariant control genes (Supplementary Table 1) and data quality was evaluated through various scatterplots [Cy3 vs. Cy5, an *R-I* (log2 ratio-intensity) plot, and *R* (log2 ratio) distribution] to assess correlation between technical replicates, dye bias, and fluorescence ratio distribution. Preprocessing analysis was carried out in InforSense, Knowledge Discovery Edition (InforSense, London, UK). The time-course data were then submitted to a mixed-model analysis of variance (ANOVA) (Sykacek et al. 2005) to select differentially expressed genes [$p < 0.05$, corrected by false discovery rate (Hochberg and Benjamini 1990)] which were grouped into nine clusters according to their gene expression profile using k-means, Pearson's correlation (Jain and Dubes 1988). The data from the germ cell-deficient models was analyzed the same way.

For a more precise refinement of cellular origin of differentially expressed genes, the germ cell-deficient models data were integrated with the first-wave data. Correlation with the presence or absence of germ cells gives an indication of somatic, germ cell, or both somatic and germ cell expression.

All genes were annotated with respect to potential biological process, molecular function, and cellular component using Onto-Express, a package based on Gene Ontology (GO) Consortium categories (Khatri et al. 2002). This allowed grouping of genes within each cluster in relation to their GO category, with the intention of revealing whether particular bioprocesses are represented in each cluster.

Library sequencing. To extend IMAGE consortium sequence data, single-pass sequencing of unsequenced clones was performed followed by Blast searches. The sequences were blasted with default parameters against the public nr database via the NCBI website (www.ncbi.nlm.nih.org/blast). Each clone was assigned an accession number corresponding to a gene that displayed an *e*-score below 1*e*-40. The choice of the clone ID was made according to the accession number quality. NM_ identifiers were preferred, followed by AK and then XM- prefixes. Where the sequence did not match any known gene, the sequence was then blasted against the EST (expressed sequences tags) database.

Real-time RT-PCR. The reactions were carried out using the quantitect SYBR green RT-PCR kit (Qiagen) according to the manufacturer's instructions. All RNA samples were adjusted to the same concentration. The reactions were incubated in the Bio-Rad iCycler (BioRad Laboratories, Hercules, CA) using the following cycling conditions: 50°C for 30 min followed by 95°C for 15 min followed by 30 cycles of 94/55/72°C for 30/30/30 sec. A melting curve was also obtained to verify the specificity and identity of the RT-PCR product. Twenty-five pairs of primers were designed to span introns to control for DNA contamination of the RNA samples (see Supplementary Table 2 for primer sequences). The genes were tested in triplicate across the first wave of spermatogenesis and for XX*Sxr*[b], *mshi*, *Bax*–/–, and *bs* mouse models using the same RNA samples used to generate the microarray data. *Beta actin* and *Rbm3* were used as invariant loading controls. The

Table 2. Proportion of clones that are downregulated, upregulated, or flat in the XX*Sxr*[b] mouse model within each cluster

	$S1_{(380)}$	$S2_{(533)}$	$PreM1_{(279)}$	$PreM2_{(365)}$	$M1_{(363)}$	$M2_{(413)}$	$PM1_{(411)}$	$PM2_{(365)}$	$PM3_{(410)}$
Down	$98_{(373)}$	$81.6_{(435)}$	$17_{(47)}$	$4_{(15)}$	$98.4_{(357)}$	$98_{(405)}$	$94_{(387)}$	$99_{(361)}$	$88_{(360)}$
Flat	$2_{(7)}$	$18_{(96)}$	$74_{(206)}$	$53_{(194)}$	$1.6_{(6)}$	$1.5_{(6)}$	$6_{(24)}$	$1_{(4)}$	$10.5_{(43)}$
Up	$0_{(0)}$	$0.4_{(2)}$	$9_{(24)}$	$43_{(156)}$	$0_{(0)}$	$0.5_{(2)}$	$0_{(0)}$	$0_{(0)}$	$1.5_{(7)}$

A cutoff of 3 SD (standard deviations) from the adult mean expression level was applied to categorize genes as downregulated, upregulated, or flat in XX*Sxr*[b] mouse model. This table indicates the proportion (%) of these three categories within the nine clusters. The total number of clones within each cluster and falling into each category is indicated in parentheses. All clusters comprise genes that are mainly underexpressed in XX*Sxr*[b] (downregulated category) except PreM1 and PreM2 clusters for which genes are mainly upregulated or flat (unaltered) in the XX*Sxr*[b] model.

transcript abundance was represented by a C_t value, the number of cycles to reach a defined intensity threshold obtained from an average of triplicate measurements. This represents the inverse of the abundance of a transcript. The adult value for each gene time point was subtracted to make it comparable with the ratio measurement used to reveal relative expression changes in the array data where the adult RNA was used as a common reference. The real-time RT-PCR expression values were plotted as an inverse of the C_t minus adult C_t value.

RNA in situ hybridisation. Isolated plasmid DNA was linearized to produce sense (Apa1) and antisense (PstI) templates purified using the minelute column purification kit (Qiagen). *In vitro* transcription was then performed using the T7/Sp6 Maxiscript kit and the DIG-labeled cRNAs synthesized were then purified on RNeasy columns (Qiagen). Using the hybridization buffer provided by the mRNA locator *in situ* hybridization kit (Ambion, Austin, TX), probes (50 ng) were applied on Bouin's fixed paraffin-embedded mouse testis sections and left to hybridize for 18 h at 55°C. Slides were washed in decreasing strengths of prewarmed SSC solutions (4 × SSC /1 mM DTT, 2 × SSC/1 mM DTT, 2 × SSC/1 mM DTT, 0.1 × SSC) at 55°C and RNase treated at 37°C. Color development was performed using the DIG nucleic acid detection kit and DIG wash and block buffer set (Roche Molecular Biochemicals, Indianapolis, IN) according to the manufacturer's protocol and nuclei staining was carried out using Mayer's hematoxylin.

Results

Transcription patterns during the first wave of spermatogenesis. Transcription profile analysis of nine time points covering the premeiosis proliferative (day 1 to day 10), meiotic (day 10 to day 19), and spermiogenic (day 19 to 8 weeks) stages (three time points per stage) of the first wave of spermatogenesis was performed using the arrays described in the *Materials and methods* section. The raw and nor-

malized data are available online via ArrayExpress accession number E-MEXP-571. Expression profiling was confirmed through parallel real-time RT-PCR analysis of the same RNA samples using a range of genes present on the array and through validation against published profiles of a large number of previously studied genes (Supplementary Table 3).

Significant differential gene expression ($p < 0.05$) was observed in 3525 clones representing 1667 unique genes plus 730 as-yet unsequenced clones. *K*-means analysis was used to partition these genes into nine broad clusters. Clusters were designated as somatic (S1, S2), premeiotic (preM1, PreM2), meiotic (M1, M2), and postmeiotic (PM1, PM2, PM3) based on the proportions of clones in each cluster derived from the different libraries in the gene set (Table 1, Fig. 1).

In contrast to our prior data (Ellis et al. 2004), many of the genes show much less variation over the first wave and a much more diffuse rise from day 1 to adult, indicating that these genes are expressed in multiple cell types. This is expected because of the use of a nonsubtracted gene set which thus includes many genes with widespread expression patterns. Nevertheless, the expression profiles for clusters assigned to germ cells are generally in good agreement with this cDNA library breakdown, with premeiotic clusters showing a rise in abundance between days 1 and 10, meiotic clusters showing a diffuse rise from days 10 to 19, and postmeiotic clusters showing a rise after day 19. The only exception to this is cluster PM1, which begins to rise from day 13 onward, indicating that these genes are expressed in meiotic and postmeiotic stages.

Surprisingly, genes in the two "somatic" clusters S1 and S2 show a clear rise across the first wave, indicating preferential expression in germ cells. This germ cell expression was confirmed by comparison to XX*Sxr*[b] and by *in situ* hybridization (see below).

Use of germ cell-deficient mouse models to assign transcripts to different testis cell types. Four germ cell–deficient mouse models with different

Table 3. List of apoptotic-related genes grouped according to the molecular pathway they are involved in and their expression pattern within the testis

	Genes	Gene expression
A	*Dap*	spg, spc, spd
	Nipa	som, *spg, spc-I*
	Api5	som, *spg, spc-I*
	Dad1	som, *spg, spc-I*
	Btg2	som, *spg, spc-I*
	Clu	som (SC; Ahuja et al. 1994)
	Uchl1	som, *spg, spc-I* (spg, SC in adult mouse testis; Kon et al. 1999)
	Pdcd5	som, *spg, spc-I*
B	**FasL**	spd (spc, spd; D'Alessio et al. 2001)
	Fas	som (SC; Riccioli et al. 2000)
	Daxx	spc, spd, som (protein in mouse SC; Lopez et al. 2002)
	Faf1	spg, spc, spd, som (human testis; Ryu et al. 1999)
	Dedd	spc-II, spd (in 21 day old rat; Leo et al. 1998)
	Casp8	Som
C	**Tnfa**	som (spc, spd, testicular macrophages; De et al. 1993)
	Tnfr1	som (LC, SC; Mauduit et al. 1996, De et al. 1993)
	Siah2	spc, spd
	Gsk3b	spc, spd (Bspg, prelepspc, lepspc, SC; Guo et al. 2003)
	Traip	som, *spg, spc-I*
	Nfkb1	spc, spd, som (rat protein in SC, pspc, spd; Delfino et al. 1998)
	Ikbb	spc, spd (spd; Budde et al. 2002)
	Eif5a	spg, spc, spd, som
D	***Bax***	som (spg, spc, SC; Krajewski et al. 1994a,b)
	Bcl2l14	spd (human testis; Guo et al. 2001)
	AK005633	Spd
	Vdac2	spg, spc, spd (late spc, spd, spz in bovine testis; Hinsch et al. 2001)
	Sod1	Som
	Diablo	spc (mainly pspc; El Chami. 2005)
	Endog	spc-II, spd (mouse testis; Zhang et al. 2003)
	Rnf7	spg, spc, spd (mouse testis; Sun et al. 2001)
	Aven	spg, spc, spd (Ina et al. 2003)
E	***Bcap31***	Som
	Bcap29	spc, spd
	Sumo1	Som, *spg, spc-I* (mouse&rat protein in all GC, SC and LC; Vigodner et al. 2005)
	Senp2	spc, *spd*
	Dap3	spc, spd

Each apoptotic-related gene has been assigned to a particular testicular cell type(s) on the basis of its expression pattern across the first wave and in the germ cell-deficient mouse models. *In situ* hybridization analysis of some genes upregulated in XX*Sxr*[b] has demonstrated that they can also be expressed in germ cells. Where upregulation in XX*Sxr*[b] is combined with a first-wave profile that correlates with particular germ cell types, the potential germ cell site of expression is indicated in italics. Genes in bold correspond to genes assayed by real-time RT-PCR only; genes in bold and underlined were tested via microarray and real-time RT-PCR techniques; genes in normal type were tested only via the microarray technique. A: genes that could not be assigned to a particular apoptotic pathway but mainly corresponded to antiapoptotic genes. B: FAS system-related genes. C: TNF pathway-related genes. D: Mitochondrial apoptotic pathway-related genes. E: Endoplasmic reticulum apoptotic pathway-related genes. In parentheses are the cell-type expression patterns reported by others. spg = spermatogonia; Bspg = type B spermatogonia; spc-I = primary spermatocytes; prelepspc = preleptotene spermatocytes; lepspc = leptotene spermatocytes; pspc = pachytene spermatocytes; spc-II = secondary spermatocytes; spd = spermatids; spz = spermatozoa; GC = germ cell; Som = somatic cells; SC = Sertoli cell; LC = Leydig cell.

germ cell content were investigated to refine assignment of differentially expressed transcripts to testis cell types. The data from the mouse models were integrated with the corresponding clustered expression profile from the analysis of the first-wave data (Fig. 2). In terms of expression levels in each germ cell-deficient model, most of the clones in any given cluster behaved as a cohort (Fig. 2). Generally, the relative expression levels correlate with germ cell content of the testes from each model; highly reduced expression levels in XX*Sxr*[b] where there are no germ cells; increased levels in *mshi* and *Bax*−/− where there are progressively more mature germ cells; and higher levels in *bs* where all germ cell types (at reduced levels compared to normal) are present. In the *mshi* and *Bax*−/− models (where there are no postmeiotic cells), expression levels are more repressed in the PM clusters than in the M clusters, confirming that PM clusters represent spermatid expression and the M clusters represent less mature stages (Fig. 2). The clones in the PreM clusters displayed mixed expression patterns across the germ
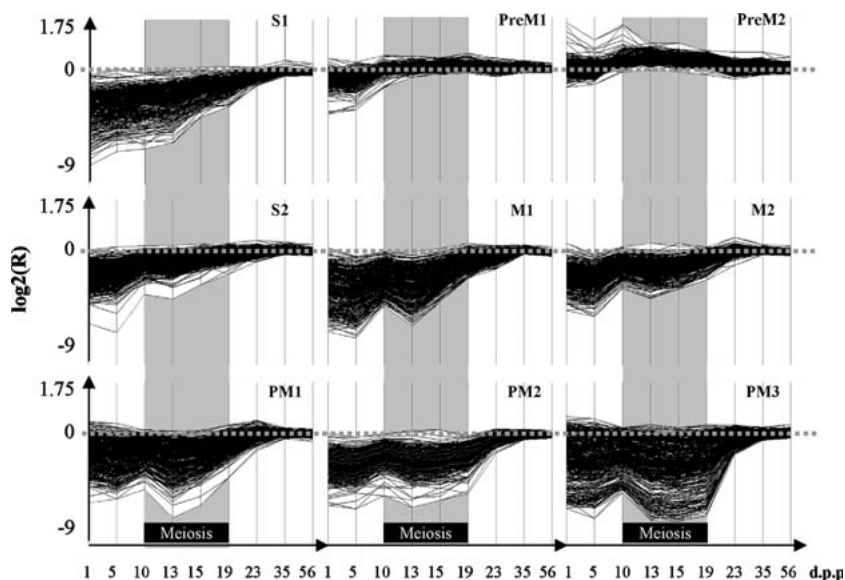
Fig. 1. Cluster gene expression patterns. Graphical representation of the differentially expressed genes ($p < 0.05$) that have been grouped into nine clusters through k-means analysis. The time points are plotted on the x axis (days 1, 5, 10, 13, 15, 19, 23, 35, 56) and gene expression relative to the 8-week-old adults (log2 transformed ratios) on the y axis (R). Following normalization to a set of controls (see Supplementary Table 1 for list), a mixed-model ANOVA was applied to select the significant genes on the basis of their p value ($p < 0.05$). K-means has partitioned the significant data into nine clusters labeled somatic (S1, S2), premeiotic (PreM1, PreM2), meiotic (M1, M2), and postmeiotic (PM1, PM2, PM3) according to the libraries from which the clones are derived (see Table 1) . The y-axis data ranges from −9 to 1.75 in all graphs. The dashed line runs through the value that corresponds to an equal expression in the juvenile and adult control mouse (log2 = 0). The S clusters exhibit a gradual increase across the first wave of spermatogenesis. PreM1 clusters show a clear rise in expression between day 5 and day 10. M clusters rise in expression throughout the period of meiosis (shaded), as does cluster PM1. PM2 and PM3 expression levels increase from day 19.

cell-deficient mouse models, particularly in XXSxr^b (Fig. 2), suggesting that these clusters include genes with several different cellular patterns of expression. Interestingly, the expression of some PreM1 and PreM2 genes is either increased (Fig. 3C) or at normal testis levels (Fig. 3A, B, D) in the *Bax* knockout model. This indicates that the expression of these genes is associated with the presence of the spermatogonia-like cells that accumulate in the *Bax*−/− model, confirming that these genes are highly expressed in early germ cell stages.

Table 2 represents the proportion of genes in each cluster that are upregulated, downregulated, or unchanged in XXSxr^b (up- and downregulation taken as ±3 SD from the mean adult expression). With the exception of the premeiotic clusters, all clusters contain a majority of genes whose expression is associated with the presence of germ cells (81.6%–99%, downregulated group) (Table 2). The PreM clusters, however, include many transcripts whose transcription is not germ cell specific. Eighty-three percent of the clones in PreM1 and 96% of the clones in PreM2 are upregulated or flat in XXSxr^b (Table 2), indicating a degree of somatic expression of these genes. This is in accordance with the results of Shima et al. (2004), who found that there were few

genes that were completely specific to early germ cell stages.

In situ *hybridization results.* *In situ* hybridizations were performed to precisely locate gene expression within the testis for the S1 and S2 Sertoli cell-derived clones that showed expression profiles suggestive of germ cell expression. In addition, genes from the premeiotic clusters that were upregulated or flat in XXSxr^b were also tested.

Sertoli cell-derived clones correspond to genes expressed predominantly in spermatocytes and round spermatids. The first-wave and germ cell-deficient models' array data indicated that many S1 and S2 Sertoli cell-derived clones were expressed in a germ cell-associated manner (gradual increase across the first wave and underexpression in XXSxr^b). *In situ* hybridization analysis for four genes (*Tctex1*, *Pscd2*, *Kars*, *Tmsb10*; Fig. 4A−D) indicated strong expression in spermatocytes and round spermatids but no detectable expression in Sertoli cell or any other somatic cell type (*Tmsb10* also shows expression in elongating spermatids; Fig. 4D).

This inconsistency between the observed expression profile and the library source of the clones
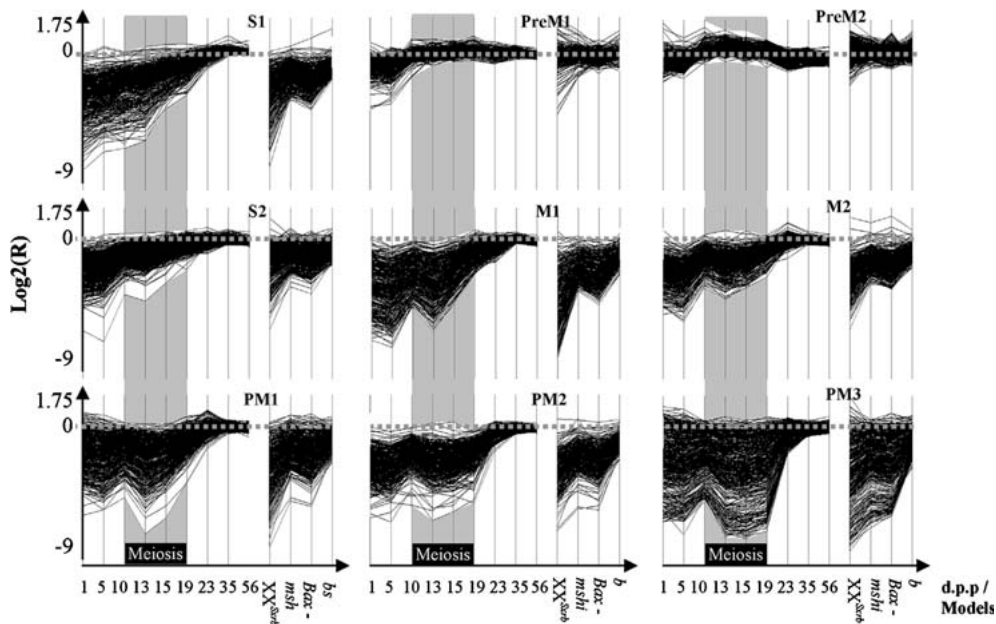
Fig. 2. First-wave data integrated with the expression ratios found in the germ cell-deficient mouse models' gene expression patterns grouped by cluster. The expression ratios found across the germ cell-deficient models for genes in each cluster have been added to the first-wave profiles. The time points and mouse models are plotted on the *x* axis (days 1, 5, 10, 13, 15, 19, 23, 35, 56, XX*Sxr*[b], *mshi*, *Bax*−/−, *bs*) and gene expression relative to the 8-week-old adults (log2 transformed ratios) on the *y* axis. The *y*-axis data ranges from −9 to 1.75 in all graphs. The dashed line runs through the value that corresponds to an equal expression in the juvenile and adult control mouse (log2 = 0).

in these clusters is a result of either cross-contamination between testis cell type during purification [∼2% for this library (McCarrey et al. 1999)] or redundant gene expression in the different germ and somatic cell types. The latter appears the more likely explanation, because the Shima et al. (2004) study also indicated that there are comparatively few Sertoli cell-specific genes. Thus, these genes are likely to be expressed in both Sertoli cells and germ cells, but at much lower levels in the former. It should also be borne in mind that the Sertoli cell library was derived from 18-day-old mice where expression levels of certain Sertoli cell genes may be higher than in the adult.

PreM clusters contain genes expressed in somatic and germ cells. The expression patterns of the PreM clusters in the germ cell-depleted models suggest that some of these genes are expressed in somatic cells and in premeiotic cell types. We tested this by RNA i*n situ* hybridization analysis for three genes showing upregulation in XX*Sxr*[b] (*Sin3b*, *Bmp9*, *Vim*; Fig. 4E−G) and three genes showing level expression in XX*Sxr*[b] (*Cnr*, *Erf1*, *Rbbp4*; Fig. 4H−J). In all cases, as expected, there was preferential expression in spermatogonia or early spermatocytes. In addition, four of the six genes (*Sin3b*, *Bmp9*, *Vim*, and *Cnr*) showed detectable expression in somatic

cell types. This demonstrates the utility of the germ cell-deficient models in revealing the somatic expression of these genes, which would not have been suspected from the first-wave profile alone.

Erf1 and *Rbbp4* transcripts (Fig. 4I, J) were not detectable in somatic cells and appear to be expressed specifically in spermatocytes. The *in situ* hybridization technique may not be sensitive enough to detect the expression of *Erf1* and *Rbbp4* in somatic cells. In addition, the warning that this technique is routinely used for qualitative rather than quantitative assessment must be borne in mind, so that these data are, in fact, a complement to extend the quantitative results of the microarray.

It is interesting to note that *Sin3b*, *Bmp9*, and *Vim* are upregulated in XX*Sxr*[b] despite being preferentially expressed in early germ cells. This may be a simple consequence of the relative cell proportions in XX*Sxr*[b] testis or, more intriguingly, may indicate inhibition of the expression of these genes in somatic cells by the presence of germ cells in normal adult testis.

Determination of biological function of differentially expressed genes based on Gene Ontology Consortium data. Onto-Express was used to assign all differentially expressed genes to a biological process, molecular function, cell component, and
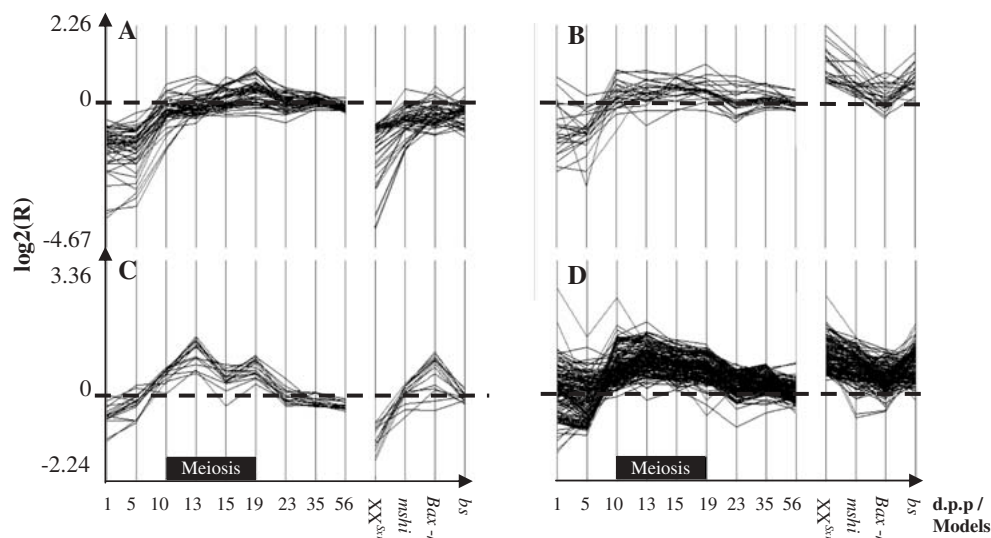
Fig. 3. Graphical representation of PreM cluster genes up- and downregulated in XX*Sxr*^{b}. Time points across the first wave and germ cell deficient mouse models are plotted on the x axis (days 1, 5, 10, 13, 15, 19, 23, 35, 56, XX*Sxr*^{b}, *mshi*, *Bax*−/−, *bs*) and gene expression relative to the 8-week-old adults (log2 transformed ratios) on the y axis. The data ranges from −4.67 to 2.26 for preM1 cluster (**A, B**). (**A**) Downregulated genes in XX*Sxr*^{b}. (**B**) Upregulated genes in XX*Sxr*^{b}. The data range from −2.24 and 3.36 for the PreM2 cluster (**C, D**). (**C**) Downregulated genes in XX*Sxr*^{b}. (**D**) Upregulated genes in XX*Sxr*^{b}. Downregulation and upregulation in XX*Sxr*^{b} were determined on a cutoff basis of 3 SD from the adult mean.

chromosome location defined by the Gene Ontology Consortium. Each cluster comprised at least 50% of sequenced genes with an unknown function, highlighting how this approach can discover novel genes potentially playing a role in spermatogenesis. On the whole, the biological processes identified for the known genes were common to all clusters but represented in different proportions. These include signal transduction, cell growth, and/or maintenance (transport, cellular organization, cell proliferation), development (morphogenesis and reproduction), and protein and DNA/RNA metabolism (Fig. 5).

Genes involved in cell organization are expressed mainly during the early and late stages of spermatogenesis, affecting cytoplasmic organization (microtubule- and actin-related genes: *Hdac6*, *Arpc5*, *Cdc42*, *Myl6*), ribosome biogenesis during premeiosis (see gene examples below), and nuclear organization (chromatin remodeling: *Prm1*, *Prm2*, *Prm3*, *Tnp1*, *Tnp2*, *Cdyl*, *Hist1h2bp*, *Hils1*) as expected in postmeiotic stages.

Meiotic genes were present mostly in cluster M1 [*Meig1* (7 clones), *tsga2* (2 clones), *Clgn*, AK016125] and mitotic genes in cluster M2 (*Cetn1*, *Mad2l2*, *Ccnk*, *Pttg1*, *Ran*), suggesting that M1 is likely to represent genes necessary for the first division of meiosis and M2 genes necessary for meiosis II. Cell proliferation appears to be primarily represented in PreM2, consistent with spermatogonial proliferation taking place at this stage [*Mif*, *cdca7*, *Erf1* (15 clones)]. DNA packaging (*Hmgn2*, *Hmga1*, *Hat1*), DNA repair

(*Xab2*, *Sumo1*), DNA replication (*Orcl6*), transcription regulation (*Cited1*, *Taf11*, *Snrpb*, *Brd7*, *Tceg1*, *Ankrd10*), and RNA processing (*Ddx20*, *Lsm4*, *Sfrs16*, *Cpsf5*) constitute the most abundant ontology categories in the PreM clusters.

Genes associated with the regulation of transcription represent a significant component of all clusters except S1, especially in PM1 (*Zbtb9*, *Znhit*, *Fank1*, *Bat4*, *Bbx*). PM1 is the cluster identified as covering the transition between meiosis and haploid stages, when many haploid-specific genes are activated. These transcriptional regulators thus constitute key candidate genes for the successful activation of the postmeiotic transcriptional program. It is interesting to note that transcription factors are also expressed at the later stages of spermatogenesis, presumably regulating the ongoing changes in transcription through spermatid development (*Tgifx*, *Egr3*, *Klf4*, *Crem*, *Preb*, *Scrad1*).

Electron transport-related genes are particularly present in PreM1 and, to a lesser extent, in S2 (*Acad9*, *Coxi1*, *Cox6c*, *Cox7c*, *Ndufb4*, *Ndufb9*, *Ndufa2*, *Ndufa11*, *Cox5a*, *Cox7a2*, *Coxvib2*) clusters. This expression pattern may reflect the presynthesis of messenger RNAs to be stored for later use in postmeiotic stages. There is a concentration of genes associated with ribosomal and protein biosynthesis in PreM1 and PreM2 clusters, perhaps in preparation for the production of a wide range of proteins necessary for the later stages of spermatogenesis (*Rps3 Rps5, Rps7, Rps8, Rps11, Rps16,*
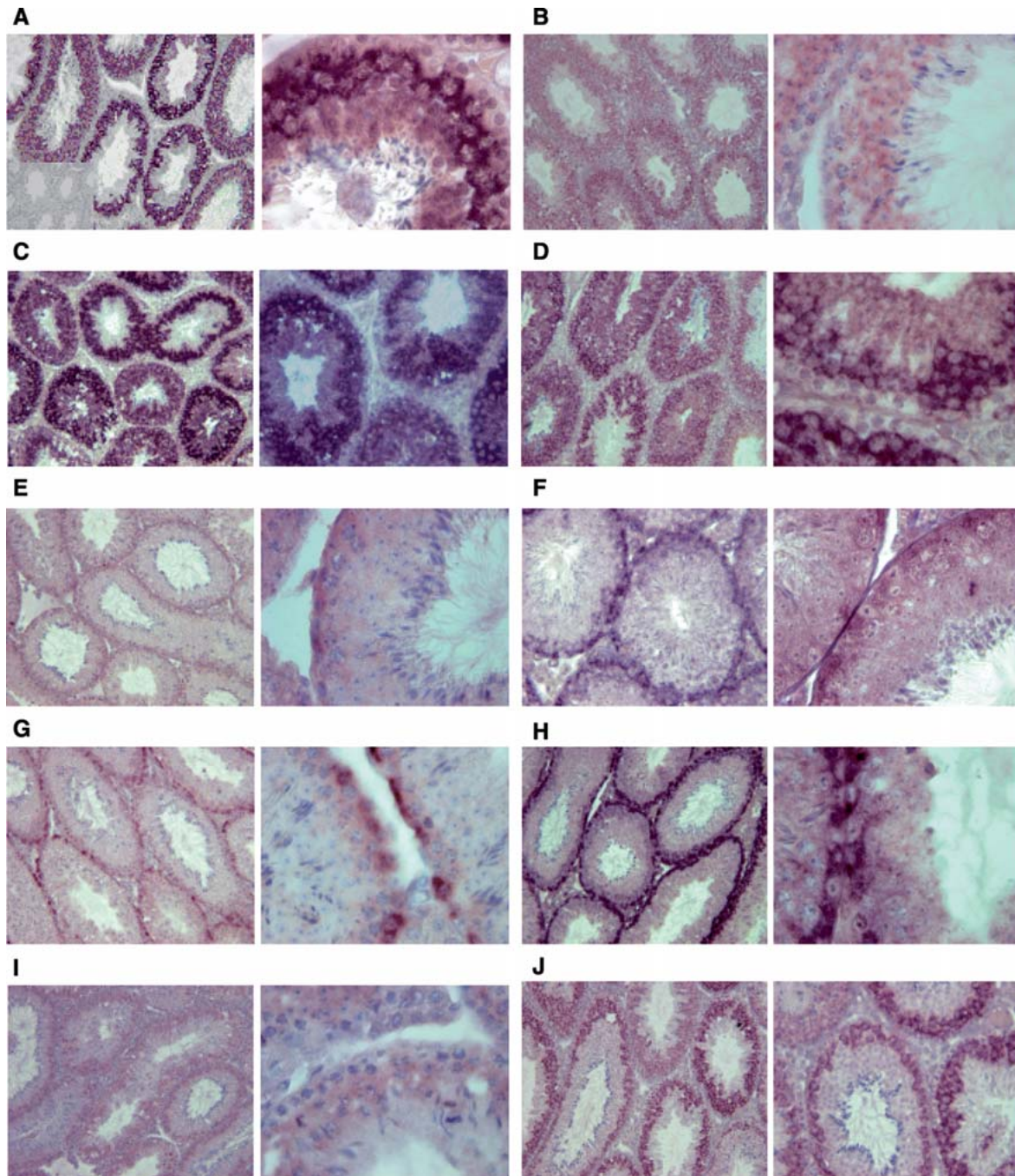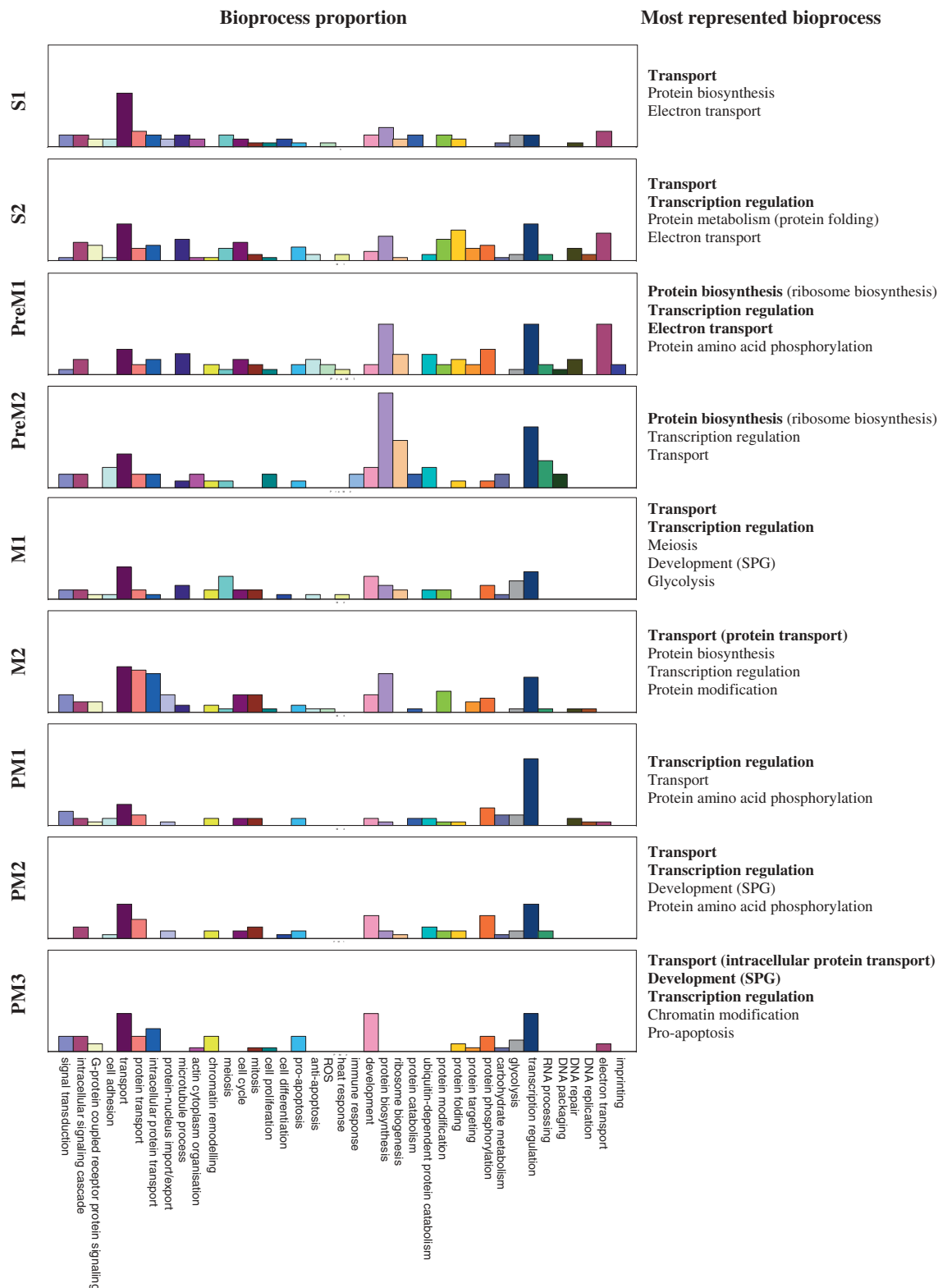
Fig. 4. *In situ* RNA results. (**A−D**) Sertoli cell-derived clones, *Tctex1, Pscd2, Kars,* and *Tmsb10,* respectively, found to be downregulated in XX*Sxr*[b] testis. All appear to be expressed in spermatocytes and round spermatids. *Tmsb10* (**D**) is also expressed in elongated spermatids. (**E−G**) *Sin3b, Bmp9,* and *Vim,* genes upregulated in the XX*Sxr*[b] mouse model that belong to the PreM clusters. Gene expression is predominant in spermatogonia and weak in early spermatocytes and Sertoli cells. *Sin3b* (**E**) also shows staining in Leydig cells. *Bmp9* (**F**) possibly has some signal in peritubular cells. *Vim* (**G**) somatic expression is restricted to Sertoli cells. (**H−J**) *Cnr, Rbbp4,* and *Erf1,* genes that also belong to the PreM clusters but whose expression is unaltered in XX*Sxr*[b]. *Cnr* (**H**) displayed a similar expression pattern as that of *Sin3b* (**E**), *Bmp9* (**F**), and *Vim* (**G**) with strong expression in spermatogonia and faint in early spermatocytes, Sertoli cells, and Leydig cells. *Rbbp4* (**I**) and *Erf1* (**J**) appear to be expressed in spermatocytes only.

Rps17, Rps21, Rps26, Rps27l, Rps29, Rpl5, Rpl14, Rpl22, Rpl27, Rpl30, Rpl31, Rpl32, Rpl35a, Rpl36, Rplp1/2, Mrpl22, Mrpl55, Ddx48, Ddx56, Eif2s2, *Eif2b1, Eif3s2*). In clusters S2 and M2, a diversity of transcripts is found to be involved, for example, in protein folding (*Cct2, Cct3, Cct4, Cct5, Cct7,*

Bioprocess proportion   **Most represented bioprocess**

S1
Transport
Protein biosynthesis
Electron transport

S2
Transport
Transcription regulation
Protein metabolism (protein folding)
Electron transport

PreM1
Protein biosynthesis (ribosome biosynthesis)
Transcription regulation
Electron transport
Protein amino acid phosphorylation

PreM2
Protein biosynthesis (ribosome biosynthesis)
Transcription regulation
Transport

M1
Transport
Transcription regulation
Meiosis
Development (SPG)
Glycolysis

M2
Transport (protein transport)
Protein biosynthesis
Transcription regulation
Protein modification

PM1
Transcription regulation
Transport
Protein amino acid phosphorylation

PM2
Transport
Transcription regulation
Development (SPG)
Protein amino acid phosphorylation

PM3
Transport (intracellular protein transport)
Development (SPG)
Transcription regulation
Chromatin modification
Pro-apoptosis

Fig. 5. Correlation of gene function with gene expression pattern. Onto-Express was used to associate the differentially expressed genes with a Gene Ontology ID to categorize genes according to their biological function. The proportion of genes associated with the different biological processes is represented by a histogram for each cluster. The bioprocesses are represented on the *x* axis and percentage on the *y* axis. All graphs are at the same scale. The most highly represented bioprocesses are indicated on the right side of the histogram.

Dnajb9, *Hspc1*), protein targeting (*Srp14*, *Srp19*), and modification (*Ubb*, *Ubc*). This may reflect subsequent processing and activation of proteins translated from mRNAs presynthesized at an earlier stage. Most transport-related genes are associated with clusters S1 and M2, consisting mainly of protein transport and particularly nuclear import/export in the latter (*Kpnb3*, *Gosr2*, *Hgs*, *Arl4*, *Kpn2*, *Kpn4*, *Kpn6*, *Tom1*, *Timm8b*). Overall, transport processes are highly represented in meiotic and postmeiotic clusters, primarily intracellular protein transport, but also ion, carbohydrate, lipid, and Golgi vesicle transport (*Rshl1*, *Sfxn1*, *Scl2a3*, *Ehd1*, *Stard6*). These functions associated with intracellular transport are likely to be particularly important in germ cells where they differentiate as a cohort in a syncytium.

Genes involved in apoptosis. Gene expression profiles for some of the cell death–elated genes found to be regulated over the first wave are represented in Fig. 6. Real-time RT-PCR was used to confirm some of the array results and was also performed on other genes involved in the pathways identified here but were not represented on the array (also in Fig. 6). The results are summarized in Table 3 together with references to related studies for all apoptotic-related genes (breakdown by pathway and cell type). Genes were assigned to spermatogonia, spermatocytes, and spermatids (according to their cluster and expression profile over the first wave and whether they were underexpressed in the XX*Sxr*[b] model). Genes that have flat expression or are overexpressed in XX*Sxr*[b] testis are expected to be expressed in somatic cells. However, from the *in situ* hybridization data on normal adult testis, some of these genes presented above are preferentially expressed in germ cells and are weak or undetectable in adult somatic cells. Thus, for XX*Sxr*[b] flat or upregulated genes, expression patterns are likely to be more complex where the normal cellular interactions are in place that can influence levels in somatic and germ cells. Consequently, it will be difficult to exclude germ cell expression or be certain of somatic cell expression levels in normal adult testis without detailed *in situ* analysis.

The relatively small number of antiapoptotic genes on the array was found mainly in premeiotic clusters and they are expressed in somatic cells (and possibly germ cells in the normal adult), based on XX*Sxr*[b] expression levels (Table 3A, *Nipa*, *Api5*, *Dad1*, *Btg2*, *Clu*). Apoptotic genes appear to be expressed at all stages (correlating with the appearance of different germ cell types) and are associated with death receptor FAS (Table 3B, *Daxx*, *Faf1*, *Dedd*, *FasL*) and TNFR1 (Table 3C, *Siah2*, *Eif5a*, *Gsk3b*)

pathways and the mitochondrial (Table 3D, *Vdac2*, *Rnf7*, *Bcl2l14*, AK005633, *Diablo*, *Aven*, *EndoG*) and endoplasmic reticulum apoptotic (Table 3E, *Bcap29*, *Senp2*, *Dap3*, *Sumo1*) pathways.

Genes involved in the FAS pathway. *Fasl* appears to be expressed in spermatids (increase at day 19, underexpression in XX*Sxr*[b]; Fig. 6A, B) whereas *Fas* is expressed in somatic cells (upregulated in XX*Sxr*[b]; Fig. 6B), most probably Sertoli cells (Riccioli et al. 2000), corroborating the work of d'Alessio et al. (2001) in rat and mouse. For each of the *Dedd*, *Daxx*, and *Faf1* genes (all FAS effectors), two clones were present on the array. Both *Dedd* clones were downregulated in XX*Sxr*[b], indicating expression in germ cells (spermatocytes and spermatids) [increase from day 15, downregulated in XX*Sxr*[b] (Fig. 6C), in agreement with previous findings in rat (Leo et al. 1998)], whereas *Daxx* and *Faf1* are expressed in germ cells and potentially in somatic cells (one clone being downregulated and the other flat in XX*Sxr*[b]; Fig. 6C). Because FASL is the trigger of the FAS pathway, it is likely that the Fas system is active during spermiogenesis.

Genes involved in the TNFa pathway. *Tnfa* expression has been previously observed in testicular macrophages, spermatocytes, and spermatids (Table 6C; De et al. 1993; Mauduit et al. 1996). *Tnfr1*, on the other hand, has been shown to be expressed in only Sertoli and Leydig cells (De et al. 1993). The real-time RT-PCR results reported here indicate *Tnfa* and *Tnfr1* are expressed in somatic cells (upregulated in XX*Sxr*[b]; Fig. 6D); this is confirmed by the drop in mRNA levels across the first wave resulting from the dilution effect contributed by increasing numbers of germ cells. *Traip* and *Gsk3b* (TNFa pathway modulators) appear to be expressed in somatic and germ cells (flat in XX*Sxr*[b]; Fig. 6E) during premeiosis and meiosis, whereas *Siah2* appears to be expressed in spermatocytes and spermatids (upregulation from day 13, downregulation in XX*Sxr*[b]; Fig. 6E). *Nfkb*, a major *Tnfa* target, displayed different expression patterns for its two isoforms: isoform 1 being restricted to germ cells (downregulated in XX*Sxr*[b]) and isoform 2 expressed in somatic cells (overexpression during the first wave and in XX*Sxr*[b]; Fig. 6F). The expression of *Ikbb* (or *Nfkbib*, an *Nfkb* inhibitor) is in germ cells (downregulated in XX*Sxr*[b]; Fig. 6F, G) possibly initiated at an early stage according to the real-time RT-PCR results, whereas the array clones display a meiotic gene expression pattern. Because *Tnfr1* is expressed only in somatic cells (De et al. 1993), the TNFa pathway appears to be triggered in somatic
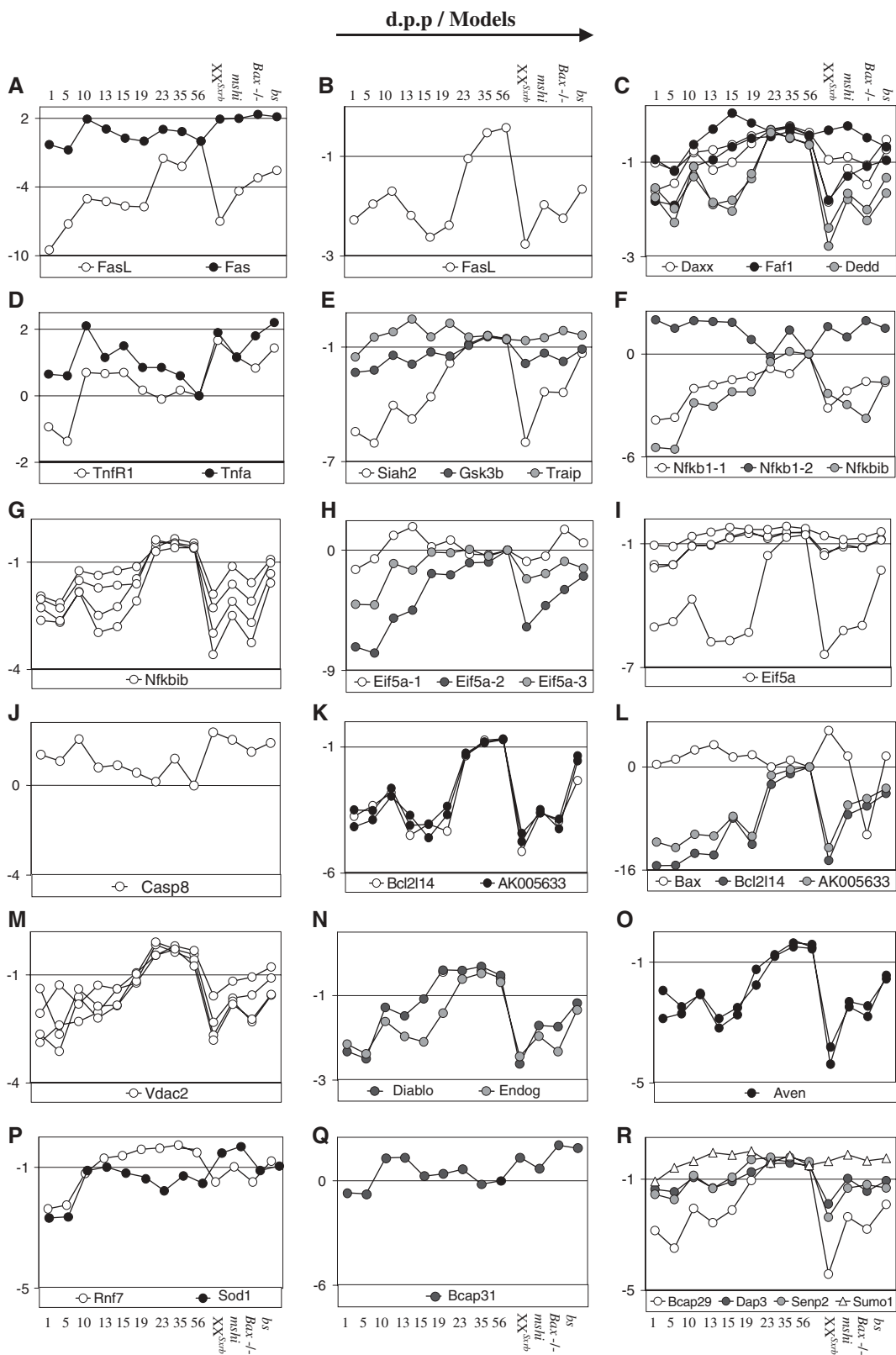
Fig. 6. Gene expression profiles of apoptotic genes generated via real-time RT-PCR and microarray techniques. In each graph, time points and germ cell-efficient mouse models are represented on the *x* axis (days 1, 5, 10, 13, 15, 19, 23, 35, 56, XX*Sxr*[b], *mshi*, *Bax*−/−, *bs*) and gene expression relative to the 8-week-old adult controls (log2 ratio) (or C_t for the real-time RT-PCR data) on the *y* axis. (**A, D, F, H, J, K, Q**) The real-time RT-PCR data (underlined). (**B, C, E, G, I, L, M, N, O, P, R**) The microarray expression profiles. AK005633 = 1700003F12Rik.

cells. The expression of TNFa modulators and *Nfkb1/Ikbb* in germ cells suggests that they might be activated by stimuli other than TNFa in the germ line. EIF5A (10 variants have been reported in total in the Ensembl database) has been shown to be up-regulated by TNFa (Taylor et al. 2004). The real-time RT-PCR data obtained for three *Eif5a* variants (primer pair 1 amplifies variant BE, pair 2 amplifies variants C and CD, pair 3 amplifies variant AE) indicated that *Eif5a* variants have different expression profiles. Variant BE seems to be specifically expressed during premeiosis and early meiosis in both germ and somatic cell components (early upregulation from day 1 to day 13 and flat in XX*Sxr^b*; Fig. 6H, *Eif5a-1*). Variant AE is expressed during premeiosis most probably in spermatogonia and primary spermatocytes (early upregulation from day 1 to day 15 and downregulated in XX*Sxr^b*; Fig. 6H, *Eif5a-3*). Expression of variants C and CD is possibly in all germ cells (gradual increase during the first wave and downregulated in XX*Sxr^b*; Fig. 6H, *Eif5a-2*). Four array clones corresponding to *Eif5a* displayed either a meiotic or a postmeiotic expression profile (downregulated in XX*Sxr^b*; Fig. 6I), none of which were in agreement with the real-time RT-PCR data. The array clones may be cross-hybridizing to other (potentially unknown) variants that do not correspond to those investigated via real-time RT-PCR. Caspase 8 is part of the initial Caspase cascade triggered by TNFa and FAS (Chen and Goeddel 2002; Los et al. 1995). Caspase 8 real-time RT-PCR data indicate a somatic expression (overexpressed during the first wave and in XX*Sxr^b*; Fig. 6J), consistent with *Tnfa* and *Fas* results.

Two Bcl-2 family members are expressed in spermatids. *Bax* expression has been previously observed in spermatognia, spermatocytes, and Sertoli cells (Krajewski et al. 1994a,b; Rodriguez et al. 1997). The real-time RT-PCR data indicate that *Bax* is expressed in somatic cells (overexpression across the first wave and in the germ cell-deficient mouse models; note its downregulation in *Bax−/−* model, as expected), which suggests an important role for *Bax* in the somatic compartment although its function has been studied mainly in germ cells (Jahnukainen et al. 2004; Nair et al. 2003; Rodriguez et al. 1997; Russell et al. 2002).

Two as-yet uncharacterized *Bcl2* family members in the mouse testis, *Bcl2l14* (or *Bcl-G*) and AK005633 (*1700003F12Rik*, hypothetical apoptosis regulator protein, *Bcl2* family BH domain-containing protein), are predicted to be expressed in spermatids by both the array and real-time RT-PCR data collected in this study (upregulation from day 19 and

underexpressed in XX*Sxr^b*; Fig. 6K, L). Other members of the apoptotic mitochondrial pathway (*Vdac2, Diablo, Endog, Aven*) appear to be expressed in spermatocytes (late spermatocytes for *Endog* and *aven*) and spermatids (upregulation from day 13−15 and downregulated in XX*Sxr^b*; Fig. 6M−O). However, *Rnf7* expression seems to be switched on in spermatogonia (early onset from day 5 and downregulated in XX*Sxr^b*; Fig. 6P). The upregulated expression of *Sod1* in XX*Sxr^b* (Fig. 6P) indicates expression in somatic cells, but the early increase in the first wave may also reflect expression in spermatogonia in normal adult testis.

ER apoptotic-related genes display a meiotic gene expression profile. The *Bcap31/Bcap29* complex has been shown to trigger the ER apoptotic pathway (Breckenridge et al. 2002). The real-time RT-PCR data indicates that *Bcap31* is expressed in somatic cells (upregulated in XX*Sxr^b*; Fig. 6Q), whereas *Bcap29* array data suggest a germ cell-predominant expression, most probably in spermatocytes and early spermatids (increase from day 13 and downregulated in XX*Sxr^b*; Fig. 6R). The *Sumo1* profile indicates expression in germ cells (early increase during the first wave and downregulated in XX*Sxr^b*; Fig. 6R). *Senp2* and *Dap3* appeared to be expressed in spermatocytes and probably in spermatids (increase from day 13 and downregulated in XX*Sxr^b*; Fig. 6R).

Genes related to cell cycle and proliferation. Based on the same reasoning used for the apoptotic genes, proliferative genes were assigned to a specific germ cell type or/and to the somatic compartment. A high proportion appears to be expressed in germ cells (downregulated in XX*Sxr^b*) and implicated in stimulating cell proliferation and progression through the cell cycle, most of which displays a meiotic expression pattern (M1 and M3 clusters). ETS-related transcription factor *Erf1*, which may be involved in cell proliferation, was found in PreM2 and appears to be expressed abundantly (15 clones). The few genes that negatively regulate cell proliferation are expressed in germ cells during late meiosis/postmeiosis (e.g., *ecgf1, Mdm2, Smarca2*; downregulated in *XXSxrb*) and possibly in both somatic and germ cells during premeiosis/early meiosis (e.g., *Ddx20, Rbbp4, Sin3b, Brd7*; upregulated or flat in XX*Sxr^b*) or in germ cells only (*Sap18, Mbd3*). Focus was toward the premeiotic proliferative genes with a view toward providing some insight into proliferation/differentiation regulation (see Table 4 for summary and Supplementary Table 5 for an extensive list of proliferative genes). Real-time RT-PCR was applied to confirm some of

Table 4. List of cell cycle/proliferation-related genes grouped according to the molecular pathway they are involved in and the cluster they belong to

Gene	Gene expression
Rbbp4	spg, spc, som [spc only by ISH], (mouse testis; Qian et al. 1995)
Erf1	spg, spc, som [spc only by ISH]
Ddx20	transcript 1: som, *spg, spc-I*; transcript 2: spd (basal germ cells, LC; Ou et al. 2001)
Sin3b	spg, spc-I, som
Sap18	spg, spc
Mbd3	spc, spd
Brd7	som, *spg, spc-I*
Mets	spg, spc
E2f1	spg, spc-I
Ccnd1	spg (gc, spg; Beumer et al. 2000)
Ccnd3	som (juvenile gc, adult spg, SC and LC; Beumer et al. 2000)
Hdac2	spg, spc-I

Each gene has been assigned to a particular testicular cell type on the basis of its expression pattern across the first wave and in the germ cell-deficient mouse models. *In situ* hybridization (ISH) analysis of some genes upregulated in XX*Sxr*^{b} has demonstrated that they can also be expressed in germ cells. Where upregulation in XX*Sxr*^{b} is combined with a first-wave profile that correlates with particular germ cell types, the potential germ cell site of expression is indicated in italics. Genes in bold correspond to genes assayed by real-time RT-PCR only; genes in bold and underlined were tested via microarray and real-time RT-PCR techniques (*Erf1* and *Rbbp4* were also assayed by ISH); genes in normal type were tested via microarray technique. In parentheses are the cell-type expression patterns reported by others. gc = gonocytes; spg = spermatogonia; spc-I = primary spermatocytes; spc-II = secondary spermatocytes; spd = spermatids; SoC = somatic cells.

these array expression profiles (*Erf1, Rbbp4, Ddx20*) and to generate data on known proliferative genes and proliferation inhibitors (*Ccnd1, Ccnd3, E2f1, Mets, Hdac2*) not represented on the arrays but involved in some of these pathways.

The array clones *Erf1, Rbbp4*, and *Ddx20* are expressed in both somatic and germ cells. The real-time RT-PCR results for *Erf1* (Ets factor 1) and *Rbbp4* (Fig. 7A, C) were in close agreement with the array data (Fig. 7B, D), indicating that their expression occurs during premeiosis and meiosis in both somatic and germ cells [flat expression of *Erf1* and *Rbbp4-1* (isoform 1) in XX*Sxr*^{b} (Fig. 7A, B), absence of expression in somatic cells as detected by *in situ* hybridization may reflect sensitivity (see above)]. *Rbbp4* isoform 2 expression appeared restricted to germ cells (downregulated in XX*Sxr*^{b}; Fig. 7C, *Rbbp4-2*).

The *Ddx20* expression profile generated via real-time PCR undergoes two phases of significant upregulation between days 5 and 10 and days 19 and 23 (Fig. 7E). However, in the microarray experiments, the *Ddx20* clones produced two divergent expression patterns (Fig. 7F). This may, therefore, represent two variant isoforms of *Ddx20*, one expressed in late spermatocytes and round spermatids and the second in somatic cells during premeiotic and meiotic stages, with the real-time RT-PCR results measuring the aggregate expression pattern of the two isoforms. However, we have as yet been unable to confirm this via *in situ* hybridization, presumably as a result of cross-hybridization.

Cell proliferation activators (*E2f1* and *Ccnd1*) and inhibitors (*Mets* and *Hdac2*) are expressed in sper-

matogonia and early spermatocytes. *E2F* is a well-known proliferative gene that is activated by Cyclin D and E gene family members (Grana et al. 1998). *E2f1* and Cyclin D isoforms 1 and 3 were tested by real-time PCR. The results indicated that *E2f1* and Cyclin D1 (Ccnd1) had very similar expression patterns suggesting a spermatogonia/early spermatocyte expression (strong expression until day 13, followed by a dilution as more mature germ cells appear and underexpression in XX*Sxr*^{b}; Fig. 7A, G). In contrast to *Ccnd1*, the high expression levels of Cyclin D isoform 3 (*Ccnd3*) in the germ cell–deficient models, including XX*Sxr*^{b}, point to a preferential somatic expression, most probably during premeotic and meiotic stages (Fig. 7G). It is suggested that *Brd7* represses ERK and Rb-E2F pathways. The array data reveal a premeiotic profile and unaltered expression in XX*Sxr*^{b}, which possibly reflects a germ cell and somatic expression.

Mets (an *Ets* inhibitor) was shown to have a role in repressing proliferation, complexed to *Ddx20* and to a histone deacetylase complex, including *Rbbp4, Sin3b*, and *Hdac2* (Klappacher et al. 2002). *Mets* and *Hdac2* real-time RT-PCR results indicated that both are probably expressed in all germ cells, but more prominently in spermatogonia and primary spermatocytes (Fig. 7E) (adult expression levels reached by day 15, underexpressed in XX*Sxr*^{b} and in near-normal levels in *Bax*–/– and *bs*). However, *Sin3b* appears to be expressed in somatic cells (upregulated in XX*Sxr*^{b}; Fig. 7H) and its known complex partner *Sap18* (Zhang et al. 1997) in germ cells (downregulated in XX*Sxr*^{b}; Fig. 7H). *Mbd3*, a member of the NURD complex (transcriptional repression complex)
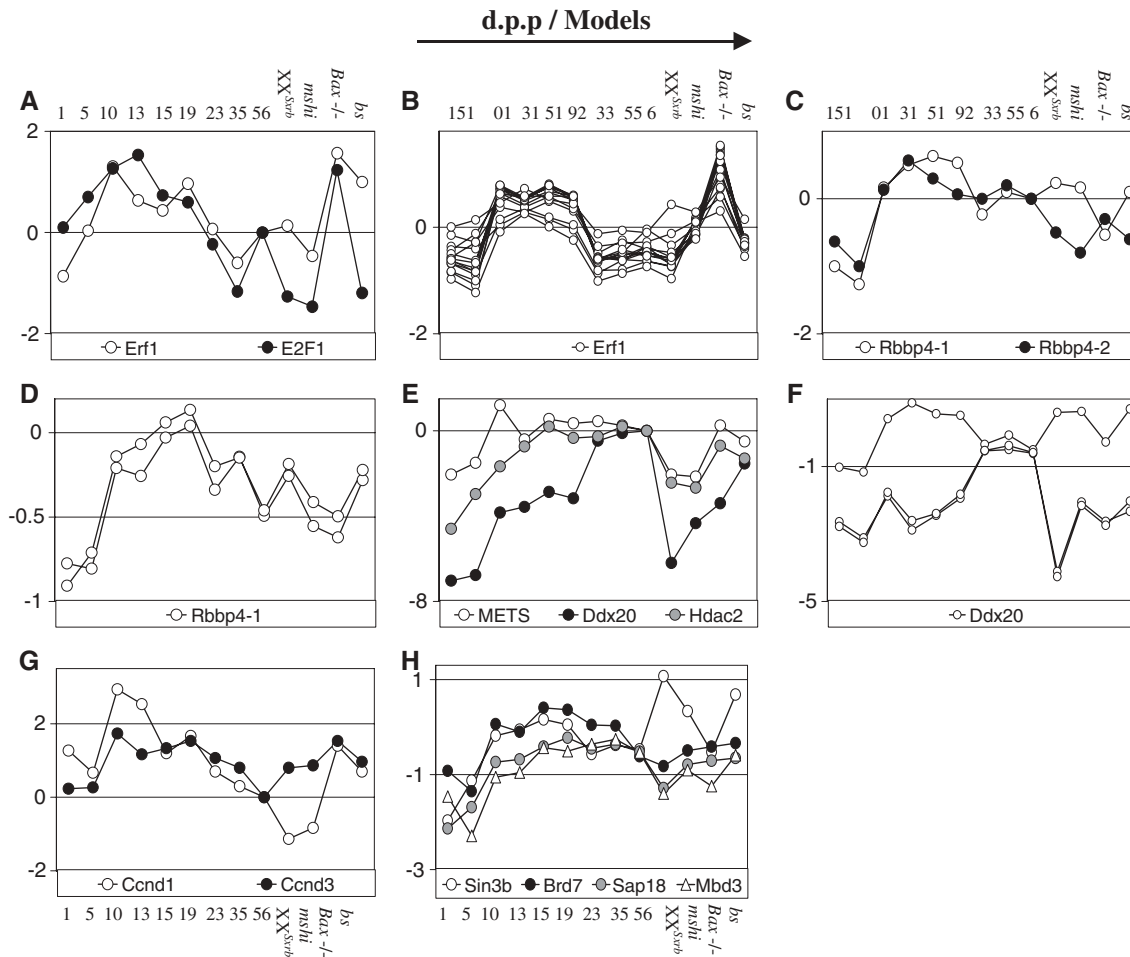
Fig. 7. Cell cycle/proliferation-related gene expression profiles generated via real-time RT-PCR and microarray analyses. In each graph, time points and mouse models are represented on the x axis (days 1, 5, 10, 13, 15, 19, 23, 35, 56, XXSxr^b, mshi, Bax−/−, bs) and gene expression relative to the 8-week-old adult controls (log2 ratio) (or C_t for the real-time RT-PCR data) on the y axis. (**A, C, E, G**) The real-time RT-PCR data (underlined). (**B, D, F, H**) The microarray expression profiles.

(Zhang et al. 1999), displayed a germ cell-dependent expression (downregulated in XXSxr^b; Fig. 7H).

Discussion

The aim of this study was to identify the cell types, stages, and genes involved in differential gene expression in the first wave of spermatogenesis and thus highlight key proteins for further investigation that are critical to the spermatogenic processes and, potentially, fertility. The choice of cDNA clones derived from purified cell-type libraries has provided a focused gene set where there is some prior knowledge of cell type of origin for transcripts. Through the inclusion of germ cell-deficient mouse models, it has been possible to refine further the assignment of transcripts to particular cell types. The microarray data has (1) identified 3525 clones representing 1667 unique genes that were regulated

during the first wave, a high proportion of which appear to be uncharacterized, (2) resolved these transcripts (through k-means cluster analysis) into nine different groups of expression patterns, and (3) allowed a correlation of these groups of expression pattern (validated through extensive real-time RT-PCR analysis and concordance with expression profiles published in the literature; see Supplementary Table 3) to particular cell types and stages.

The comparison of data from the germ cell-deficient mouse models and first wave to distinguish between genes preferentially expressed in germ and somatic cell types or both has allowed the subgrouping of genes in the premeiotic clusters likely to be involved in premeiotic and early meiotic stages. The presence within the somatic and spermatogonia/early spermatocytes gene lists of transcripts previously assigned to Sertoli cells (*Clu, Cyst9, Defb19, Serpina5, Amhr2*; see Supplementary Table

3 of references) and spermatogonia (*Ott*, *Piwil2*, *Dnmt3b*, *Scyp3*, *Tex101*) support our findings with respect to up- or downregulation in XX*Sxr*^{b} testis. The RNA *in situ* hybridization data revealed an interesting additional class of transcripts in which there is upregulation in XX*Sxr*^{b} testis but clear expression in spermatogonia and weaker expression in early spermatocytes and somatic cells (e.g., *Sin3b*, *Bmp9*, *Vim*). The explanation for their upregulation in XX*Sxr*^{b} could simply reflect the difference in testis cell content between the wild-type and XX*Sxr*^{b} models. A second explanation could be that these genes are repressed by germ cells in the wild-type mouse testis. This would be consistent with the important role that Sertoli cells play in regulating spermatogonial proliferation and differentiation. In turn, germ cells could inhibit Sertoli cell signaling, this acting as a feedback loop to control the above biological process. The various subgroups of somatic and spermatogonial genes identified through the use of germ cell-deficient models and RNA *in situ* hybridization analysis in premeiotic clusters are listed in Supplementary Table 4.

It is intriguing to observe that a large proportion of the Sertoli cell transcripts appear to be expressed in germ cells (underexpressed in XX*Sxr*^{b} and in four cases located to round spermatocytes and spermatids by *in situ* hybridization; *Tctex1*, *Pscd2*, *Kars*, *Tmsb10*) but are not detectable in somatic cells. McCarrey et al. (1999) state that the 18-day Sertoli cell library is 98% pure and thus it is unlikely that contamination explains why so many genes (about 82%) from this library show germ cell-related expression. It is possible that these genes may be expressed in both compartments and that the failure to detect these transcripts in adult Sertoli cells by *in situ* hybridization reflects ubiquitous expression but with a predominance in germ cells. It will be important to determine the level of these transcripts in 18-day Sertoli cells relative to germ cells. Many of the genes identified in this class have a transport function within the cell and thus may have an important role in the bidirectional crosstalk between Sertoli cells and associated germ cells where, at each maturation stage, specific signaling systems trigger the synthesis and release of the required nutrients and factors (Griswold 1995; Saunders 2003). It is interesting to note that for both of the S clusters there are distinct sets of genes that appear to be expressed in both somatic and germ cell compartments. This may reflect the stage-specific activity of different genetic networks in the basal and adluminal compartments and it will be important to investigate the potential role of these genes in Sertoli cell-germ cell inter-

action. The higher level of expression in germ cells may be indicative of presynthesis of these transcripts for use in later postmeiotic haploid cells and the lower efficiency of translation found in meiotic and haploid cells than in somatic cells (Kleene 2003, 2005).

The association of each gene to its Gene Ontology ID facilitates the identification of events that characterize the three stages of spermatogenesis. Premeiosis is characterized by an early and massive synthesis of ribosomal constituents, illustrating the considerable need of the seminiferous tubule cells to produce proteins. The high proportion of electron transport genes also switched on at this stage confirms that mitochondria are especially important during spermatogenesis to provide not only energy for the cell to function properly but also to ensure motility (and hence fertility) in mature sperm. Interestingly, the genes related to these two processes are primarily transcribed early in spermatogenesis. This suggests that these transcripts are likely to be stored and translated according to cellular needs during the later spermatogenic stages.

Transport and transcription regulation are the most prominent biological processes at all stages, indicating the necessity for constant delivery of new proteins to their site of action in growing and dividing germ cells and the importance of transcription regulation throughout spermatogenesis. The finding of numerous transcription factors in the late postmeiotic clusters suggests the necessity of transcripts, including transcription factors, to be present in the spermatozoa either for its further maturation in the epididymal duct or perhaps as a paternal contribution to the egg as suggested by Herrada and Wolgemuth (1997).

Taken together, the gene ontology results suggest that many so-called "housekeeping" functions, such as protein synthesis, folding, and transport, and metabolic functions, such as electron transport, are in fact coordinately regulated throughout spermatogenesis. While the functional import of these regulatory events is not fully clear, the observation that many components of given protein complexes are coregulated (e.g., chaperonins, ribosomal proteins, elongation factors, and transporters) provides fertile ground for future investigation into the mechanisms of coordinated transcriptional control.

In this study particular attention has been given to cell apoptosis and cell proliferation pathways that are important in cell number regulation. Our data for *Fas* and *Tnfa* receptor mRNAs suggest that they are expressed in somatic cells rather than in germ cells, which is consistent with published data (D'Alessio et al. 2001; De et al. 1993). FAS has been suggested to

play a role in the disease autoimmune orchitis by causing Sertoli cell apoptosis and hence leakage across the blood-testis barrier (Waldner et al. 1997). Study of the signaling pathway that is possibly involved showed that TNFa activated *Fas* expression through NFKB in mouse Sertoli cells, which would initiate Fas-mediated apoptosis in the same cell line (Starace et al. 2003). Germ cell apoptosis is still poorly understood and the involvement of the TNF and Fas systems in this process awaits further clarification. Combination of the array and real-time RT-PCR data has also indicated that variants of *Nfkb* and its inhibitor *Ikb* (and others such as *faf1, daxx, Eif5a*) are expressed in germ and somatic cells. This further supports the idea that activity of apoptotic pathways in different testis cell types depends on the combination of the expression of different variants to determine which pathway is triggered.

CASP8 performs a key role in all the apoptotic pathways identified in this study. CASP8 is activated by FAS and TNFa to initiate directly or indirectly (via Bcl2 family members and the endoplasmic reticulum *bcap31* gene) the apoptotic caspase cascade (Colussi and Kumar 1999). Our results indicate that in addition to *Fas* and *Tnfr1*, *Casp8*, *Bcap31*, and *Bax* appeared to be expressed in somatic cells. To date, apoptosis has been studied primarily in germ cells and, therefore, it would be important to understand the activity of these pathways in more detail in testicular somatic cells.

Bcl-xl and *Diva* are the only known Bcl2 members expressed in spermatids (Krajewski et al. 1994a,b; Inohara et al. 1998). The data in this article indicate a possible role for two other spermatid-specific Bcl2 family members [*Bcl2l14* and AK005633 (1700003F12Rik)] in apoptosis during spermiogenesis. BCL2L14, also named BCL-G, is predominantly expressed in human testis (Guo et al. 2001). BCL-G has two BH domains (BH2 and BH3 with opposite apoptotic functions) and is likely to have weak apoptotic properties as suggested for its human homolog (Guo et al. 2001). The function of AK005633 (*1700003F12Rik*) has not yet been studied in the testis. Spermatids undergo very low levels of apoptosis, but a number of studies have identified heat and estrogen as apoptotic triggers in these postmeiotic cells (Nair and Shaha 2003). This apoptotic activity is likely to function as a quality control measure by removing severely abnormal spermatids and thus may be induced only by strong stimuli. The hypothesized weak apoptotic properties of BCL-G would ensure a minimized cell death rate and that maturing germ cells would undergo apoptosis only in extreme cases of dysfunction and structural abnormality.

The antiapoptotic (*Rnf7, Aven*) and proapoptotic modulators (*Diablo*) of the mitochondrial pathway (Duan 1999; Chau et al. 2000; Verhagen et al. 2000) displayed different expression patterns, suggesting that germ cell apoptosis or survival could be favored depending on the presence of these factors at particular stages of spermatogenesis. Interestingly, the ENDOG caspase-independent apoptotic pathway (Li et al. 2001) is most likely to be induced in late spermatocytes and in spermatids and may represent an alternative quality control pathway.

Many genes belonging to the premeiotic and somatic clusters are associated with cell cycle and proliferation. They appear to be part of the same genetic network identified so far in macrophages (Klappacher et al. 2002), where it has been suggested that the RB-E2F pathway and SIN3B-HDAC complex act in concert to repress cell growth (stimulated by the ERK cascade) during macrophage terminal differentiation. We suggest that this molecular pathway is activated before meiosis, either in somatic cells, in Sertoli cells, or in both.

Specifically, between days 5 and 10 postpartum, we observe upregulation of the mitogenic *Ets* transcriptional suppressor (METS), together with coordinated upregulation of interacting partner genes *Sin3b, Hdac2, Rbbp4*, and *Ddx20*. This time period coincides with both the period of juvenile Sertoli cell proliferation and differentiation and a period of spermatogonial proliferation and commitment to meiosis. The growth promoters *Erf1* and *E2F1* show a similar expression pattern, suggesting that the switch from proliferation to differentiation in either or both cell types may be finely tuned by the balance of these two opposing pathways.

We propose that a histone deacetylase complex that includes HDACs, RBBP4, and SIN3B would be able, by forming a bigger complex with METS-DDX20, to inhibit transcription of ETS and E2F targets by chromatin modification, leading to inhibition of cell proliferation. Possibly some signal emitted by the differentiating cells could act as a negative feedback to initiate cell growth repression and allow terminal differentiation. In immature Sertoli cells, this pathway may also interact with the ERK proliferative cascade, which is known to be triggered in these cells by FSH (Orth 1984), leading to activation of cyclin D1 and E2F (Crepieux et al. 2001).

Our results give clues to the similarities and differences between the different cellular compartments. In particular, some genes are expressed as different isoforms in the two lineages: *Ccnd3, Rbbp4-1* in somatic cells and *Ccnd1, Rbbp4-2* in germ cells. As noted above, similar isotype variation

may be occurring for *Ddx20*, though this needs to be confirmed. Other genes in this pathway appeared to be expressed primarily in germ cells (*Mets*, *E2f1*, *Hdac2*, *Sap18*, *Mbd3*), in somatic cells (*Sin3b*), or in both somatic and germ cells (*Erf1*, *Brd7*). This potentially affects the balance between proliferation and differentiation for each cell type and may be important in adjusting the proportion of cell types in the testis.

In summary, the data generated by our microarray, real-time PCR, and *in situ* hybridization experiments have identified a candidate pathway for control of the switch between proliferation and differentiation in somatic and germ cells. Further RNA *in situ* and immunohistochemical investigations will be necessary to pin down the dynamics of this control system in somatic and spermatogonial cells.

Acknowledgments

References

1. Braun RE (1998) Post-transcriptional control of gene expression during spermatogenesis. Semin Cell Dev Biol 9, 483–489
2. Breckenridge DG, Nguyen M, Kuppig S, Reth M, Shore GC (2002) The procaspase-8 isoform, procaspase-8L, recruited to the BAP31 complex at the endoplasmic reticulum. Proc Natl Acad Sci USA 99, 4331–4336
3. Chau BN, Cheng EH, Kerr DA, Hardwick JM (2000) Aven, an novel inhibitor of capsase activation, binds Bcl-xL and Apaf-1. Mol Cell 6, 31–40
4. Chen G, Goeddel DV (2002) TNF-R1 signaling: a beautiful pathway. Science 296, 1634–1635
5. Chubb C (1989) Genetically defined mouse models of male infertility. J Androl 10, 77–88
6. Cohen PE, Pollard JW (2001) Regulation of meiotic recombination and prophase I progression in mammals. BioEssays 23, 996–1009
7. Colussi PA, Kumar S (1999) Targeted disruption of caspase genes in mice: What they tell us about the functions of individual caspases in apoptosis. Immunol Cell Biol 77, 58–63
8. Cooke HJ, Saunders PT (2002) Mouse models of male infertility. Nat Rev Genet 3, 790–801
9. Crepieux P, Marion S, Martinat N, Fafeur V, Vern Y, et al. (2001) The ERK-dependent signalling is stage-specifically modulated by FSH, during primary Sertoli cell maturation. Oncogene 20, 4696–4709
10. D'Alessio A, Riccioli A, Lauretti P, Padula F, Muciaccia B, et al. (2001) Testicular FasL is expressed by sperm cells. Proc Natl Acad Sci USA 98, 3316–3321
11. De SK, Chen HL, Pace JL, Hunt JS, Terranova PF, et al. (1993) Expression of tumor necrosis factor-alpha in mouse spermatogenic cells. Endocrinology 133, 389–396
12. Duan H, Wang Y, Aviram M, Swaroop M, Loo JA, et al. (1999) SAG, a novel zinc RING finger protein that protects cells from apoptosis induced by redox agents. Mol Cell Biol 19, 3145–3155
13. Eddy EM (2002) Male Germ Cell Gene Expression. Recent Prog Horm Res 57, 103–128
14. Ellis PJI, Furlong RA, Wilson A, Morris S, Carter D, et al. (2004) Modulation of the mouse testis transcriptome during postnatal development and in selected models of male infertility. Mol Hum Reprod 10, 271–281
15. Ellis PJ, Clemente EJ, Ball P, Toure A, Ferguson L, et al. (2005) Deletions on mouse Yq lead to upregulation of multiple X- and Y-linked transcripts in spermatids. Hum Mol Genet 14, 2705–2715
16. Grana X, Garriga J, Mayol X (1998) Role of the retinoblastoma protein family, pRB, p107 and p130 in the negative control of cell growth. Oncogene 17, 3365–3383
17. Griswold MD (1995) Interactions between germ cells and Sertoli cells in the testis. Biol Reprod 52, 211–216
18. Guo B, Godzik A, Reed JC (2001) Bcl-G, a Novel Pro-apoptotic member of the Bcl-2 family. J Biol Chem 276, 2780–2785
19. Handel M (1987) Genetic control of spermatogenesis in mice. Results Probl Cell Differ 15, 1–62
20. Hecht NB (1998) Molecular mechanisms of male germ cell differentiation. BioEssays 20, 555–561
21. Herrada G, Wolgemuth DJ (1997) The mouse transcription factor Stat4 is expressed in haploid male germ cells and is present in the perinuclear theca of spermatozoa. J Cell Sci 110, 1543–1553
22. Hochberg Y, Benjamini Y (1990) More powerful procedures for multiple significance testing. Stat Med 9, 811–818
23. Holdcraft RW, Braun RE (2004) Hormonal regulation of spermatogenesis. Int J Androl 27, 335–342
24. Inohara N, Gourley TS, Carrio R, Muniz M, Merino J, et al. (1998) Diva, a Bcl-2 homologue that binds directly to Apaf-1 and induces BH3- independent cell death. J Biol Chem 273, 32479–32486
25. Jahnukainen K, Chrysis D, Hou M, Parvinen M, Eksborg S, et al. (2004) Increased apoptosis occurring during the first wave of spermatogenesis is stage-specific and primarily affects midpachytene spermatocytes in the rat testis. Biol Reprod 70, 290–296
26. Jain AK, Dubes RC (1988) *Algorithms for Clustering Data* (Englewood Cliffs, NJ: Prentice–Hall)

27. Khatri P, Draghici S, Ostermeier G, Krawetz S (2002) Profiling gene expression using onto-express. Genomics 79, 266–270

28. Klappacher G, Lunyak V, Sykes D, Sawka-Verhelle D, Sage J, et al. (2002) An induced Ets repressor complex regulates growth arrest during terminal macrophage differentiation. Cell 109, 169–180

29. Kleene KC (2003) Patterns, mechanisms, and functions of translation regulation in mammalian spermatogenic cells. Cytogenet Genome Res 103, 217–224

30. Kleene KC (2005) Sexual selection, genetic conflict, selfish genes, and the atypical patterns of gene expression in spermatogenic cells. Dev Biol 277, 16–26

31. Knudson C, Tung K, Tourtellotte W, Brown G Korsmeyer S (1995) Bax-deficient mice with lymphoid hyperplasia and male germ cell death. Science 6, 96–99

32. Krajewski S, Krajewska M, Shabaik A, Miyashita T, Wang HG, et al. (1994) Immunohistochemical determination of in vivo distribution of Bax, a dominant inhibitor of Bcl-2. Am J Pathol 145, 1323–1336

33. Krajewski S, Krajewska M, Shabaik A, Wang HG, Irie S, et al. (1994) Immunohistochemical analysis of in vivo patterns of Bcl-X expression. Cancer Res 54, 5501–5507

34. Leo CP, Hsu SY, McGee EA, Salanova M, Hsueh AJ (1998) DEFT, a novel death effector domain-containing molecule predominantly expressed in testicular germ cells. Endocrinology 139, 4839–4848

35. Li LY, Luo X, Wang X (2001) Endonuclease G is an apoptotic DNase when released from mitochondria. Nature 412, 95–99

36. Los M, Van de Craen M, Penning LC, Schenk H, Westendorp M, et al. (1995) Requirement of an ICE/CED-3 protease for Fas/APO-1-mediated apoptosis. Nature 375, 81–83

37. Maratou K, Forster T, Costa Y, Taggart M, Speed RM, et al. (2004) Expression profiling of the developing testis in wild-type and Dazl knockout mice. Mol Reprod Dev 67, 26–54

38. Mauduit C, Besset V, Caussanel V, Benahmed M (1996) Tumor necrosis factor alpha receptor p55 is under hormonal (follicle-stimulating hormone) control in testicular Sertoli cells. Biochem Biophys Res Commun 224, 631–637

39. Mazeyrat S, Saut N, Grigoriev V, Mahadevaiah SK, Ojarikre OA, et al. (2001) A Y-encoded subunit of the translation initiation factor Eif2 is essential for mouse spermatogenesis. Nat Genet 29, 49–53

40. McCarrey JR, O'Brien DA, Skinner MK (1999) Construction and preliminary characterization of a series of mouse and rat testis cDNA library. J Androl 20, 635–639

41. McLaren A, Monk M (1981) X-chromosome activity in the germ cells of sex-reversed mouse embryos. J Reprod Fertil 63, 533–537

42. Meehan T, Schlatt S, O'Bryan MK, de Kretser DM, Loveland KL (2000) Regulation of germ cell and Sertoli cell development by activin, follistatin, and FSH. Dev Biol 220, 225–237

43. Nair R, Shaha C (2003) Diethylstilbestrol induces rat spermatogenic cell apoptosis in vivo through increased expression of spermatogenic cell Fas/FasL system. J Biol Chem 278, 6470–6481

44. Orth JM (1984) The role of follicle-stimulating hormone in controlling Sertoli cell proliferation in testes of fetal rats. Endocrinology 115, 1248–1255

45. Pawlowski WP, Cande WZ (2005) Coordinating the events of the meiotic prophase. Trends Cell Biol 15, 674–681

46. Poccia D (1986) Remodeling of nucleoproteins during gametogenesis, fertilization, and early development. Int Rev Cytol 105, 1–65

47. Riccioli A, Starace D, D'Alessio A, Starace G, Padula F, et al. (2000) TNF-alpha and IFN-gamma regulate expression and function of the Fas system in the seminiferous epithelium. J Immunol 165, 743–749

48. Rodriguez I, Ody C, Araki K, Garcia I, Vassalli P (1997) An early and massive wave of germinal cell apoptosis is required for the development of functional spermatogenesis. EMBO J 16, 2262–2270

49. Russell LD, Chiarini-Garcia H, Korsmeyer SJ, Knudson CM (2002) Bax-dependent spermatogonia apoptosis is required for testicular development and spermatogenesis. Biol Reprod 66, 950–958

50. Saunders PT (2003) Germ cell-somatic cell interactions during spermatogenesis. Reprod Suppl 61, 91–101

51. Schultz N, Hamra FK, Garbers DL (2003) A multitude of genes expressed solely in meiotic or postmeiotic spermatogenic cells offers a myriad of contraceptive targets. Proc Natl Acad Sci USA 100, 12201–12206

52. Sha J, Zhou Z, Li J, Yin L, Yang H, et al. (2002) Identification of testis development and spermatogenesis-related genes in human and mouse testes using cDNA arrays. Mol Hum Reprod 8, 511–517

53. Shima JE, McLean DJ, McCarrey JR, Griswold MD (2004) The murine testicular transcriptome: characterizing gene expression in the testis during the progression of spermatogenesis. Biol Reprod 71, 319–330

54. Starace D, Riccioli A, D'Alessio A, Giampietri C, Petrungaro S, et al. (2004) Characterization of signaling pathways leading to Fas expression induced by TNF-alpha: pivotal role of NF-kappaB. FASEB J 19, 473–475

55. Sykacek P, Furlong RA, Micklem G (2005) A friendly statistics package for microarray analysis. Bioinformatics 21, 4069–4070

56. Taylor CA, Senchyna M, Flanagan J, Joyce EM, Cliche DO, et al. (2004) Role of eIF5A in TNF-α-mediated apoptosis of lamina cribrosa cells. Invest Ophthalmol Vis Sci 45, 3568–3576

57. Toure A, Clemente EJ, Ellis P, Mahadevaiah SK, Ojarikre OA, et al. (2005) Identification of novel Y chromosome encoded transcripts by testis transcriptome analysis of mice with deletions of the Y chromosome long arm. Genome Biol 6, R102

58. Varnum D (1983) Blind-sterile: a new mutation on chromosome 2 of the house mouse. J Hered 74, 206–207

59. Verhagen AM, Ekert PG, Pakusch M, Silke J, Connolly LM, et al. (2000) Identification of DIABLO, a mammalian protein that promotes apoptosis by binding to and antagonizing IAP proteins. Cell 102, 43–53

60. Waldner H, Sobel RA, Howard E, Kuchroo VK (1997) Fas- and FasL-deficient mice are resistant to induction of autoimmune encephalomyelitis. J Immunol 159, 3100–3103

61. Ward-Bailey P, Johnson K, Handel M, Harris B, Davisson M (1996) A new mouse mutation causing male sterility and histoincompatibility. Mamm Genome 7, 793–797

62. Wrobel G, Primig M (2005) Mammalian male germ cells are fertile ground for expression profiling of sexual reproduction. Reproduction 129, 1–7

63. Zhang Y, Iratni R, Erdjument-Bromage H, Tempst P, Reinberg D (1997) Histone deacetylases and SAP18, a novel polypeptide, are components of a human Sin3 complex. Cell 89, 357–364

64. Zhang Y, Ng HH, Erdjument-Bromage H, Tempst P, Bird A, et al. (1999) Analysis of the NuRD subunits reveals a histone deacetylase core complex and a connection with DNA methylation. Genes Dev 13, 1924–1935